This is the peer-reviewed version of the following article:

1   **LIPIDS COMPOSITION OF THE MICROBIAL MAT FROM HYPERSALINE**

2   **ENVIRONMENT (VERMELHA LAGOON, RIO DE JANEIRO, BRAZIL)**

3   Tais Freitas da Silva[a,*], Sinda Beatriz Carvalhal Gomes[b], Frederico Sobrinho da Silva[b],

4   Ksenija Stojanović[c], João Graciano Mendonça Filho[b], Milton Santos[b]

5   [*]Corresponding author: tais.freitas@ufrgs.br

6

7   *[a] Department of Geology, Institute of Geosciences, Federal University of Rio Grande do Sul,*

8   *Avenida Bento Gonçalves 9500 Prédio 43126 Sala 201, CEP 91509-900 Porto Alegre, Brazil*

9   *[b] Department of Geology, Institute of Geosciences, Federal University of Rio de Janeiro, Av.*

10   *Athos da Silveira, 274, prédio do CCMN, Sala J1020, Campus Ilha do Fundão, CEP 21949-*

11   *900 Rio de Janeiro, RJ, Brazil*

12   *[c] University of Belgrade, Faculty of Chemistry, Studentskitrg 12-16, 11000 Belgrade, Serbia*

13

14   **Abstract**

15   The paper is aimed to determine the sources of organic matter (OM) and to check the

16   capability of lipid compounds for distinguishing different color layers of a stratified

17   hypersaline microbial mat. The relation of precursor lipids from microbial mat to

18   hydrocarbons composition in fossil records was also evaluated. For that purpose, composition

19   of glycolipids (GLs), phospholipids (PLs) and "neutral" lipids (NLs, including hydrocarbons,

20   *n*-alkanols, sterols, hopanols, free fatty acids and wax esters) in 4 different color layers (A-D;

21   depth intervals: up to 0.5 cm, 0.5-1.0 cm, 1.5-3.0 cm and 3.0-6.0 cm, respectively) of a

22   stratified hypersaline mat from the Vermelha lagoon, Rio de Janeiro, Brazil was studied.

23   Microscopic characterization revealed the presence of 16 cyanobacterial

24   morphospecies, with predominance of *Microcoleus chthonoplastes*. The notable prevalence of

25   saturated straight-chain fatty acids (FAs), *n*-16:0 and *n*-18:0 and their monounsaturated

26 counterparts, n-16:1 and n-18:1 in all three lipids fractions (GLs, PLs and NLs), associated

27 with domination of n-C_{17} alkane and n-$C_{17:1}$ alkene among the hydrocarbons confirmed the

28 main imprint of cyanobacteria. The composition of studied lipid classes implies the

29 contribution of sulfate-reducing bacteria such as *Desulfomicrobium sp.* strain, purple sulfur

30 bacteria, as well as possible input of *Geobacter spp.* and *Desulfovibrio spp.*, particularly in

31 deeper layers.

32   The notable decrease in total extractable lipids (TELs) yield from A to D layer

33 indicates that lipid synthesis is much more intense by photosynthesizing cyanobacteria than

34 by anaerobic microorganisms. The content of PLs was uniform and low (<5%) in all layers

35 implying their extremely quick degradation. GLs, following by NLs were most abundant in

36 all layers indicating the medium which is characterized by excess of the carbon source and the

37 limited nitrogen source which regulates microorganisms' growth. Upper layers, A (green) and

38 B (reddish-brown) differ from the lower ones, C (dark brown greenish) and D (brown)

39 according to the NLs/GLs ratio which is higher in former.

40   The lipids composition reveals distinctions between individual layers within microbial

41 mat well. The observed layers clearly differ according to amount of high molecular weight

42 (C_{22}-C_{31}) n-alkanes and long-chain (C_{21}-C_{30}) n-alkanols, content of phytol, bishomohopanol,

43 tetrahymanol, C_{27}-C_{29} sterols, the stanol/stenol ratio in the neutral lipid fraction, as well as the

44 content of branched (*iso* and *anteiso*) FAs and w9/w7 FA ratio in the GLs fraction. Mentioned

45 parameters imply a greater contribution of sulfate-reducing and purple sulfur bacteria to layer

46 B, higher impact of photosynthetic red algae in upper layers A and B, the elevated

47 contribution of marine ciliate species, feeding on bacteria to layers B and C, as well as the

48 increment of anoxygenic phototrophic and heterotrophic bacteria to layer D. The greatest

49 capability for hydrocarbons synthesis is observed in layer B.

50   The composition of lipid classes in microbial mat showed a significant relationship

51   with most important biomarkers' fingerprints in the source rocks extracts and petroleums

52   derived from carbonate hypersaline environments, including distribution of *n*-alkanes, high

53   abundance of phytane and gammacerane, as well as distribution of C_{27}-C_{29} regular steranes.

54

55   Keywords: microbial mat, hypersaline environment, cyanobacteria, "neutral" lipids,

56   glyclolipids, phospholipids.

57

58   **INTRODUCTION**

59   Lipid biomarkers have been used as powerful tool in the characterization of microbial

60   community structure in microbialites (Kaur *et al.*, 2011). For example, archaeal and bacterial

61   lipid distributions and carbon isotopic composition have proved effective in the

62   characterization of mat-building organisms in geothermal systems, and to microbial

63   communities in cold seep carbonates.

64   Microbial mats are laminated biofilms that grow mostly on submerged or moist

65   surfaces. They usually develop in heat- and/or salinity-stressed habitats and the organisms are

66   often spatially organized as a result of physicochemical gradients (Pierson *et al.*, 1994;

67   Rontani and Volkman, 2005; Sánchez *et al.*, 2006). They generally are composed of few

68   groups of microbes: cyanobacteria, colorless sulfur bacteria, purple sulfur bacteria and

69   sulfate-reducing bacteria (Boudou *et al.*, 1986; Dobson *et al.*, 1988; van Gemerden, 1993).

70   The lower diversity of species of these ecosystems provides qualitative differentiation of the

71   sources of autochthonous (bacterial, algal and macrophytes) from allochthonous organic

72   matter (OM) in sediments and the recognition of early diagenetic processes, which can be

73   used for biogeochemical modeling studies (Grimalt *et al.,* 1992).

74   In mats the activities of bacteria involve complex syntrophic communities in which

75   photosynthesis in the upper mat is balanced by decomposition below (Grimalt *et al.*, 1992).

76   The result is a well-defined stratified benthic community with aerobic phototrophs

77   (cyanobacteria) in the near surface, anoxygenic phototrophs below, followed by

78   chemoorganotrophs that require neither oxygen nor light (Riding, 2000). Therefore, their

79   individual layers tend to be populated by specific organisms (e.g. cyanobacteria, purple

80   photosynthetic bacteria, sulfate-reducing bacteria) which allow that differences in the OM of

81   various mat horizons can be assess in terms of the contributions from, and effects of these

82   different microorganism (Boudou *et al.*, 1986).

83   Since modern microbial mats have been considered as analogues for ancient

84   sediments, the bacterial activates have been studied by lipids, which are biomolecules that

85   have greater preservation potential and therefore are more easily preserved over geological

86   timescales (Riding, 2000; Plet *et al.*, 2018). Lipid analysis have been used for identification of

87   specific microbial group from a variety of localities and environmental settings (Navarrete *et*

88   *al.*, 2000; Bühring *et al.*, 2009; Allen *et al.*, 2010; Pagès *et al.*, 2014; Plet *et al.*, 2018).

89   In lipid studies, three subdivisions are recognized: "neutral" lipids (NLs), glycolipids

90   (GLs) and phospholipids (PLs) (Kates, 1972). The "neutral" lipids include aliphatic

91   hydrocarbons, wax esters, free fatty acids, free sterols and free alcohols. The wax esters and

92   free fatty acids (FAs) are common storage lipids in protozoa and eukaryotic algae (Piorreck

93   and Pohl, 1984), whilst free sterols are ubiquitous in all organisms other than bacteria. GLs

94   are sugar-containing lipids which are more polar than PLs and are abundant constituents of

95   many gram-positive bacteria and some gram-negative bacteria. However, algae and higher

96   plants also produce GLs (Lechevalier and Moss, 1977). On the other hand, PLs are membrane

97   constituents of all organisms (Gillan and Sandstrom, 1985).

98   In view of these, we focus in the distribution and composition of NLs (free FAs,

99   hydrocarbons, *n*-alkanols, sterols, hopanols, wax esters) and methyl esters of FAs obtained by

100   methanolysis of GLs and PLs in microbial mat from the hypersaline Vermelha lagoon, Rio de

101   Janeiro, Brazil, which could improve the understanding of biosignatures in the pre-salt

102   petroleum reservoir.

103   Although, numerous researches have been done studies of this lagoon with focus in

104   geology, biology, taxonomy and geochemistry (Knoppers and Kjerfve, 1999; van Lith *et al.*,

105   2002; Silva E Silva *et al.*, 2004, 2005; Silva and Carvalhal, 2005; Damazio and Silva E Silva,

106   2006; Laut *et al.*, 2017; Ramos *et al.*, 2017; Rocha and Borgui, 2017), this paper represents

107   probably one of the first reports about determination and quantification of the polar lipids

108   composition, testing the capability of these biomolecules for distinguishing individual layers

109   within microbial mat. Furthermore, it is well known that source rock kerogen, which is a

110   heterogeneous, polymeric material formed from a biomass consisting of variable proportions

111   of the remains of algae, higher plants and bacteria (Tissot and Welte, 1984) represents the

112   main precursor of petroleum via the geothermal maturation. The contribution of algae and

113   higher plants to sedimentary OM is well documented using microscopic techniques (e.g.

114   maceral composition) and biomarkers patterns (*n*-alkanes, steroids, gymnosperm derived

115   diterpenoids,   angiosperm   derived   non-hopanoid   triterpenoids,   botryococcane,

116   polymethylsqualanes; Peters *et al*., 2005), whereas evidence for a contribution from bacteria

117   is usually referred to presence of hopanoids (Nytoft, 2011). Therefore, the second objective of

118   the study was to connect the composition of precursor lipids in microbial mats with

119   composition of ancient biomarkers commonly present in source rocks extracts and

120   petroleums, which provides the essential data for the better understanding of the

121   transformation of microbial OM during sedimentation processes and its contribution to fossil

122   records.

123

MATERIAL AND METHODS

Study Area

126   The Vermelha lagoon ("Lagoa" Vermelha) is a shallow, hypersaline and carbonaceous

127   coastal lagoon at southeast coast of the state of Rio de Janeiro, Brazil. It is approximately 4.5

128   km long and 250 to 850 m wide, covering an area of 1.90 km^2 with a mean water depth of 2.0

129   m. The Vermelha lagoon is situated between two parallel dune systems, the younger

130   (Holocenic) which separates it from the Atlantic Ocean and the older (Pleistocenic) which

131   separates it from the much larger lagoon, Araruama lagoon (Fig. 1) (van Lith *et al.*, 2002).

132   There is no surface drainage in the lagoon environment, hence the water balance is

133   controlled by weather conditions (dry or rainy season). The underground inflow of ground

134   waters and sea conditions promote seepage, which can considerably increase the lagoon's

135   water volume. The water body is fragmented in almost five interconnected ponds with

136   different dimensions arising from decades of salt explorations (Knoppers and Kjerfve, 1999).

137   High salinity, sulfate reducing bacterial activity, indicated by the presence of sulfide

138   and positive $\delta^{34}S$ of sulfate, and biotic/abiotic sulfide oxidation are the main controls on

139   dolomite formation in sediments (van Lith *et al.*, 2002; Moreira *et al.*, 2004). This special

140   mineralogical composition of sediments is in contrast with the neighboring lagoons where

141   detrital sedimentation predominates (Vasconcelos *et al.*, 2006).

142   Living microbial mats and stromatolites have beam described for the Vermelha lagoon

143   in areas that are flooded periodically or intermittently, such as intertidal or adjacent supratidal

144   environments like temporary pools (Silva E Silva *et al.*, 2004; Silva E Silva and Carvalhal,

145   2005).

146

147

148   *Sampling*

149   Mat sample was collected in the intertidal region at a small central pond of the

150   Vermelha lagoon which is bordering of saltpans (Fig. 2). The mat was classified in

151   morphotype, according to its geometry, texture and color at the sampling site. The sample was

152   collected using a metal spatula, placed into aluminum container and was refrigerated during

153   transport.

154   Sample was characterized regarding cohesion, inner lamination and color zonation by

155   stereoscopic microscopy, and then cut in four intervals according to color, and freeze-dried

156   for lipid analyses. For cyanobacterial analyses the mat was preserved in formaldehyde

157   solution (4%).

158

159   *Cyanobacterial Identification*

160   Emphasis was put on the cyanobacterial taxa, which are key organisms and that

161   dominate the biomass of mat (Dijkman *et al.*, 2010). Slides from mat were observed

162   microscopically (Axiovision Imager.A1 Zeiss), approximately ten, to ensure a good overall

163   representation of resident morphotypes. The taxonomic identification was carried out in

164   accordance with traditional morphological features.

165

166   *Lipid Analysis*

167   The layers of mat were extracted with a solvent mixture dichloromethane/methanol

168   (2:1, v/v) using an Accelerator Solvent Extractor (ASE). The extracts were fractionated using

169   benzenesulfonic acid bonding Solid Phase Extraction (SPE) columns (DSC-SCX; 500 mg, 3

170   cm^3). The fractions were eluted sequentially with dichloromethane, acetone and methanol to

171   obtain neutral lipids, glycolipids and phospholipids fractions, respectively. The neutral lipids

172   were fractionated using column chromatography (5 g silica-gel 60, 63-200 µm, dried at 110

173 ºC for 8 h) and five fractions were eluted with 10 cm^3 *n*-hexane, 9 cm^3 *n*-

174 hexane/dichloromethane, 10 cm^3 dichloromethane, 10 cm^3 dichloromethane/acetone and 15

175 cm^3 dichloromethane/methanol yielding, respectively: F1 containing hydrocarbons, F2

176 containing ketones, F3 containing esters, F4 containing sterols and alcohols and F5 containing

177 acidic compounds. Fractions were concentrated by rotary evaporation. After solvent

178 evaporation, the residues of fractions F4 and F5 were taken up in 100 μl of BSTFA (Supelco)

179 and silylated for 1 h at 50 ºC.

180   Glycolipids and phospholipids fractions were saponified by heating process at 100 ºC

181 in a water bath in the presence of 0.5 cm^3 of methanol/toluene (1:1, v/v) and 0.5 cm^3 of

182 potassium hydroxide/methanol (0.2 mol/dm^3). After cooling 1.5 cm^3 of BF$_3$/methanol was

183 added and subsequently extraction was performed four times with *n*-hexane. The combined *n*-

184 hexane extracts were concentrated.

185   All fractions were analyzed by gas chromatography-mass spectrometry (GC-MS). The

186 GC-MS analyses were performed using an Agilent Technologies instrument (from USA)

187 comprising a 7890A model gas chromatograph equipped with a 7693 auto sampler and

188 coupled to a triple quadrupole 7000B Mass Spectrometer (MS). Helium was the carrier gas, in

189 constant flow mode, at 1.2 cm^3/min. A DB-1 column (100% dimethylpolysiloxane, 30 m-

190 long, with 0.25 mm inner diameter and 0.25 μm film thickness) was used. The column was

191 heated from 40ºC (1 min, hold) to 140ºC at a rate of 20ºC/min and then to 280ºC at 2ºC/min.

192 The final temperature of 280°C was maintained for an additional 30 minutes. The injector and

193 transfer line temperatures were 280ºC. The MS was operated under the following conditions:

194 the ion source temperature was 290ºC, the interface temperature was 300ºC and the

195 quadrupole temperature was 150ºC. Electron impact ionization (70eV) was used and full scan

196 spectra were obtained by scanning *m/z* 50-800 at 1 scan s^{-1}. The compound assignment was

197 performed by examination and comparison with literature mass spectra and NIST (National

198 Institute of Standards and Technology) library. The quantitative analyses were performed by

199 comparison of peak areas of the compounds with those of internal standards: deuterated

200 tetracosane for hydrocarbons analysis and 5α-androstan-3β-ol for alcohols, free fatty acids,

201 wax esters and fatty acid methyl esters (FAMEs).

202

203   **RESULTS**

204   *Mat Description and Cyanobacterial Diversity*

205   Polygonal mats were found at intertidal region of the Vermelha lagoon. External

206 morphology showed traditional features like upturned crack margins producing saucer-shaped

207 polygons, with approximately 50 cm of width and almost 6 cm of thickness. This mat had a

208 flat dark pigmented green surface and internally was subdivided into 4 different colors layers.

209 The top of mat showed a green layer (0.5 cm), followed by a reddish-brown layer (0.5-1.5

210 cm), a dark brown greenish layer (1.5-3.0 cm) and finally a thicker bottom brown layer (3.0-

211 6.0 cm), which are assigned as A, B, C and D, respectively. Irregular and thin carbonate

212 laminations were mainly observed in the brown layer (D).

213   These color stratifications are linked to position of different microorganism guilds in

214 response to physiological requirements (gradients of light, oxygen, redox potential, sulfide

215 and pH) as described by (Visscher *et al.*, 1992; Ward *et al.*, 1998; Stolz, 2000). The

216 positioning and morphology of microbial mat agreed with classifications proposed for others

217 hypersaline environments (Horodyski and Bloeser, 1977; Silva E Silva *et al.*, 2005). The

218 occurrence of the same cyanobacterial mat in the neighbor lagoons of Araruama system was

219 previously described (Silva E Silva *et al.*, 2005; Damazio and Silva E Silva, 2006; Ramos *et*

220 *al.*, 2017; Rocha and Borgui, 2017).

221   The cyanobacteria diversity comprises sixteen morphospecies: *Aphanocapsa litoralis;*

222 *Aphanothece marina; Aphanothece salina; Chroococcus membraninus; Chroococcus minor;*

223 *Chroococcus turgidus; Gloeocapsopsis crepidinum; Gomphosphaeria aponina;*

224 *Gomphosphaeria salina; Johannesbaptita pellucida; Synechococcus salinarum; Jaaginema*

225 *subtilissimun; Microcoleus chthonoplastes; Microcoleus tenerrimu; Phormidium okeni and*

226 *Spirulina subsalsa.*

227   Some morphoespecies detected such as *Microcoleus, Schizothrix, Spirulina,*

228 *Aphanothece, Aphanocapsa, Chroococcus, Gloeocapsopsis, Synechococcus,*

229 *Johannesbaptistia* are known for their tolerance to desiccation and elevated salinities and

230 have been reported from hypersaline mats, lagoons and inland evaporitic lakes (Abed and

231 Garcia-Pichel, 2001; Jonkers *et al.*, 2003; Richert *et al.*, 2006; Abed *et al.*, 2008, 2015;

232 Ramos *et al.*, 2017). *Microcoleus chthonoplastes* was the dominant cyanobacteria in this mat

233 and other hypersaline mats, pointing out to its importance in the formation and stabilization of

234 this mat morphology (Garcia-Pichel *et al.*, 1996).

235

236   *Total Extractable Lipids*

237   According to the literature, in shallow aquatic environments where sunlight is

238 available, the lipids from uppermost layers of microbial mats represent inputs of aerobic

239 photosynthesizing cyanobacteria and other oxygenic prototroph while the lipids from lowest

240 layers represent different types of anaerobic bacteria.

241   The yields of total extractable lipids (TELs) were 14.73, 6.84, 3.88 and 1.14 mg/g$^-$

242 (dry mat) to layer A, B, C and D, respectively. Glycolipids (GLs) constituted the major

243 compounds present in all layers, comprising from 55.40% of TELs in the layer A to 89.30%

244 of TELs in the layer C. The proportion of neutral lipids (NLs) of the microbial mat analyzed

245 was 41.01%, 28.67%, 8.84% and 17.37% of TELs in the layers A, B, C and D, respectively.

246 The content of phospholipids (PLs) was uniform and low (< 5%) in all layers (Fig. 3).

247

248   ***Neutral Lipids***

249   Compounds in the neutral lipids (NLs) fraction include hydrocarbons, free fatty acids

250   (FFAs), sterols, hopanols, wax esters and alcohols (*n*-alkanols, *n*-alkenols and alcohols with

251   branched isoprenoid chain) (Table 1).

252   Free fatty acids (FFAs) dominated in all layers, with exception of layer D, which is

253   characterized by uniform concentration of FFAs and hydrocarbons (Table 1). Content of

254   hydrocarbons is two orders of magnitude higher in layer B than in other layers (Table 1),

255   which may be attractive for consideration of biotechnological hydrocarbons producing from

256   renewable sources, similar to those from *Botryococcus braunii* (Banerjee *et al*., 2002).

257   Alcohols are more abundant than sterols and hopanols in layers A and D, whereas sterols

258   prevail over alcohols and hopanols in layers B and C. Interestingly, contents of all three

259   compound classes show the same trend versus depth/layers (Table 1). The hopanol

260   concentration (C_{32} hopanol, with ββ-configuration) increases in layers B and C, which

261   indicates bacterial community changes. The increase of hopanol concentration in layers B and

262   C is associated with rise of sterols concentration (Table 1) that suggests higher contribution of

263   eukaryotic organisms.

264   Wax esters are identified in low amount and exhibit decreasing trend from top to

265   bottom, being absent in the deepest layer D (Table 1).

266

267   **Hydrocarbons**

268   *n*-Alkanes ranged from *n*-C_{17} to *n*-C_{35}, having maximum at *n*-C_{17}, were detected in

269   concentrations of 3.95, 44.09, 0.77 and 1.57 µg/g dry mat in layers from A to D, respectively.

270   The abundance of high molecular weight (HMW) *n*-alkanes (>*n*-C_{21}) was lowest at the

271   surface (0.01 µg/g dry mat, layer A) and increased with depth to a maximum at 0.5-1.5 cm

272   (1.53 µg/g dry mat, layer B), but decreased at 1.5-3 cm (0.19 µg/g dry mat, layer C) and

273   increase again to 0.77 µg/g dry mat (layer D), below 3 cm.

274   Phytane (C_{20} regular isoprenoid) was detected in the range 0.27 - 17.10 µg/g dry mat,

275   with the highest concentration in layer B and the lowest concentration in layer A. Another

276   important isoprenoid biomarker, β-carotane was identified exclusively in layers A and B in

277   relatively low concentration 0.82 and 0.54 µg/g dry mat, respectively. The absence of this

278   biomarker in lower layers can be attributed to diagenetic alteration of the sensitive carotenoid

279   skeleton and/or absence of its precursors.

280   Pentacyclic terpenoid hydrocarbons with hopanoid skeleton, 22,29,30-trisnorhop-

281   17(21)-ene, 17β(H)-22,29,30-trisnorhopane, hop-17(21)-ene, and hop-22(29)-ene (diploptene)

282   were present with total concentrations of 0.37, 0.28, 0.03 and 0.22 µg/g dry mat, in layers A

283   to D, respectively (Fig. 4). These compounds are synthesized by a wide variety of aerobic (i.e.

284   methanotrophs, heterotrophs and cyanobacteria) and anaerobic bacteria including strictly

285   anaerobic bacteria capable of anaerobic ammonium oxidation (Rohmer *et al.*, 1984; Volkman

286   *et al.*, 1986; Venkatesan, 1988; Ourisson and Rohmer, 1992; Summons *et al.*, 1994;

287   Sinninghe Damsté *et al.*, 2004).

288

289   **Free Fatty Acids**

290   Free fatty acids (FFAs) have been used in studies of microbial mats as biomarkers for

291   different bacterial groups and they reflect the adaptation of bacteria to environmental stress

292   (Grimalt *et al.*, 1992; Abed *et al.*, 2008; Scherf and Rullkötter, 2009). Distributions of FFAs

293   vary as a function of their source and branched short-chain (C_{15} and C_{17}) are considered as

294   "typical bacterial" free fatty acids (Rütters *et al.*, 2002). However, long-chain fatty acids (C_{20}-

295   C_{30}) are produced by many organisms; they may derive either directly from higher land plant

296   material (such as cuticular waxes) or from eroded peats (Lehtonen and Ketola, 1993). In

297   addition, even-numbered long-chain fatty acids have also been discovered in some soil

298   bacteria (Řezanka *et al.*, 1991) and in *Desulfotomaculum sp*. (Řezanka *et al.*, 1990).

299   FFAs are dominant NLs components showing, as total lipiids, notable decrease of

300   concentration with depth (from 1234.73 µg/g dry mat in layer A to 4.72 µg/g dry mat in layer

301   D; Table 1). In the layer A, FFAs are detected in range C_{12}-C_{24}; layer B is characterized

302   exclusively by presence of short chain (C_{12}-C_{19}) FFAs, whereas in layers C and D, FFAs are

303   observed in range from C_{12} to C_{30}. The ratio of short- (C_{14}-C_{20}) vs. long-chain saturated FFAs

304   (C_{21}-C_{30}) showed the following values: 4.16 (layer C), 32.28 (layer D), 83.81 (layer A),

305   associated with the presence of short-chain FFAs up to C_{19} only in layer B, implies marked

306   prevalence of the former, particularly in upper layers. Saturated straight-chain FFAs 16:0 and

307   18:0 and their monounsaturated counterparts 16:1 and 18:1 dominated all layers and

308   accounted for relative amounts from 60 to 75% of total fatty acids. The most dominant FFA

309   was *n*-16:0 which made up ca. 31% of total fatty acids in layer A, 46% in the layer B, 31% in

310   the layer C, and 52% in the layer D. The amount of the fatty acid *n*-18:0 ranged between

311   4.13% and 18.81%, being the lowest in layer A and the highest in layer D, respectively.

312

313   **Normal, Isoprenoid and Pentacyclic Triterpenoid Alcohols, Steroids**

314   Straight chain fatty alcohols (C_{14}-C_{30}), exhibiting a strong even over odd

315   predominance, which resulted in CPI values ranged from 0.01 (layers C and D) to 0.03 (layer

316   A), are present in all layers, but greater concentration is observed in upper layers A and B

317   (20.07 and 20.42 µg/g dry mat, respectively; Table 2). *n*-Alkanol maximum in layers A and D

318   corresponds to *n*-18:0, whereas the most abundant homologues in layers B and C are *n*-28:0

319   and *n*-24:0, respectively. Content of long chain (C_{21}-C_{30}) *n*-alkanols increases from layer A to

320   layer C, showing the maximum in layer B. The ratio of short to long-chain *n*-alkanols

321   displayed notable decrease from layer A (1.94) to deeper layers where comparable values

322   (0.76-0.90) are observed (Table 2).

323   Branched alcohols with isoprenoid skeleton, phytol and isophytol are present in all

324   layers, with concentrations varying from 0.01 to 2.22 µg/g dry mat and from 0.03 to 2.53 µg/g

325   dry mat. The content of both compounds is the lowest in layer D and the highest layer B

326   (Table 2), which has the highest amount of phytane.

327   The C_{27}-C_{29} sterols, exhibiting the prevalence of C_{29} homologue, are present in all

328   samples, with the highest concentration (21.27 and 26.07 µg/g dry mat) in layers B and C

329   (Table 2). These sterols, however, are not specific to cyanobacteria and their occurrence in the

330   mat layers could be contributions from other eukaryotic aquatic microorganisms and higher

331   plants. Unsaturated stenols, with maximum at C_{29} 24-ethylcholest-5-en-3β-ol, prevail over

332   saturated stanols in the cyanobacterial mat layer A, whereas in deeper layers, B and C the

333   opposite trend is observed, with maximum at 5α(H)-24-ethylcholestan-3β-ol (Table 2).

334   Pentacyclic triterpenoid alcohols, bishomohopanol (0.12-6.06 µg/g dry mat) and

335   tetrahymanol (0.02-2.72 µg/g dry mat) are observed in all layers (Table 2). The concentrations

336   of both, bishomohopanol and tetrahymanol are higher in layers B and C than in layer A, and

337   particularly layer D. Bishomohopanol is probably derived from microbial degradation of the

338   bacteriohopanetetrols (BHPs) of cyanobacteria. Tetrahymanol has been found in sediments

339   from a variety of depositional environments, as well as in bacterial/algal mats (Venkatesan,

340   1989), but higher concentration of this compound usually typifies the interface between oxic

341   and anoxic zones in stratified water columns (Sinninghe Damsté *et al*., 1995).

342

343   ***Glycolipids and Phospholipids***

344   The bound fatty acids (FAs) from saponification of the glycolipids (GLs) and

345   phospholipids (PLs) fractions are typically inferred to derive from the hydrolysis of 1,2-

346 diacylglycoglycerolipids and 1,2-diacylglycerophospholipids respectively. FAMEs are

347 derived from alkaline methanolysis of intact polar lipids of the PLs and GLs fractions. Both

348 individual FAMEs and their characteristic distributions can be useful biomarkers for diverse

349 groups of organisms in environmental samples (Allen *et al.*, 2010).

350 Mass chromatograms (*m/z* 74) of methanolysis products of GLs and PLs fractions are

351 presented in Figures 5 and 6, respectively. Mass chromatograms indicate that methanolysis

352 products of GLs and PLs fractions obtained from the same mat are not similar in composition.

353 FAMEs from GLs fractions showed presence of saturated, branched and monounsaturated

354 compounds (Fig. 5), while FAMEs from PLs fractions almost all comprise *n*-16:0 and *n*-18:0

355 (Fig. 6).

356 Normal FAMEs were the most abundant in GLs fractions of all layers, with

357 concentrations from 47.19 μg/g dry mat (layer B) to 72.30 μg/g dry mat (layer C). They are

358 identified in range from *n*-13:0 to *n*-18:0, with *n*-17:0 being absent. The branched acids are

359 represented by C_{14}-C_{17} compounds, showing maximum at *iso*-15:0 in all samples, and having

360 the highest concentration in layers B and D (Fig. 5; Table 3). The presence of

361 monounsaturated FAMEs, *n*-16:1, *n*-18:1 and *n*-19:1 is also noticed within the GLs fraction of

362 all layers. The concentration of monounsaturated FAMEs decreases with depth (Table 3).

363

364 **DISCUSSION**

365 *The Capability of Polar Lipids Composition for Distinguishing Individual Layers within*

366 *Microbial Mat*

367 **Total Extractable Lipids**

368 Notable decrease in TELs content from A to D layer indicates that lipid synthesis is

369 much more intense by aerobic than by anaerobic microorganisms. The prevalence of GLs and

370 NLs in all layers (Fig. 3) can be indicative for the medium which is characterized by excess of

371   the carbon source, whereas the nitrogen source limits microorganisms' growth (Alvarez and

372   Steinbüchel, 2002; Alvarez, 2003). High amounts of GLs indicate a high contribution of

373   photosynthetic organisms to microbial mat. Also, the microbial community of natural

374   environments is frequently exposed to many fluctuating conditions, as variation of

375   temperature. In these cases, the microorganisms may accumulate GLs as energy source,

376   allowing their survival in these variable conditions. Upper layers of microbial mats differ

377   from the lower ones according to NLs/GLs ratio which is higher in former (Fig. 3), indicating

378   more intense synthesis/accumulation of NLs by aerobic than by anaerobic microorganisms.

379

380   **Neutral Lipids**

381   The prevalence of n-C$_{17}$ n-alkane associated with prominent n-C$_{17:1}$ alkene is typical

382   for cyanobacteria (Thiel *et al.*, 1997), and was also previously reported in hypersaline, hot

383   springs, and freshwater microbial mats (Grimalt *et al.*, 1992; Fourcans *et al.*, 2004; Rontani

384   and Volkman, 2005; Scherf and Rullkötter, 2009). The result is in accordance with

385   domination of *Microcoleus* taxon in studied mat. Despite the prevalence of n-heptadecane in

386   all layers, they can be distinguish by Carbon Preference Index (CPI), reflecting the ratio of

387   odd/even n-alkanes, and the concentration of high molecular weight (HMW) n-alkanes (C$_{22}$-

388   C$_{31}$). CPI showed values of 1.26, 5.21, 1.99 and 3.61 in layers A, B, C and D, respectively.

389   The highest content of HMW n-alkanes, associated with the highest amount of long-chain

390   (C$_{21}$-C$_{30}$) n-alkanols in layer B (Table 2) can be attributed to greater contribution of *Spirulina*

391   (Franco *et al.,* 2016), which presence is confirmed in the mat, as well as to sulfate-reducing

392   and heterotrophic bacteria. The highest impact of sulfate-reducing bacteria to layer B is

393   further supported by the highest ratio of hop-17(21)-ene and hop-22(29)-ene (Wolff *et al.*,

394   1992) exhibiting the value of 1.42, 1.84, 1.22 and 0.92 for layer A, B, C and D, respectively.

395   The increase in content of HMW n-alkanes in the deepest layer D may be indicative for

396 anoxygenic phototrophic and heterotrophic bacteria, and it is consistent with rise of content of

397 C_{27} hopanoids, particularly 17β(H)-22,29,30-trisnorhopane (Fig. 4).

398 The greater content of phytol in upper layers A and B (Table 2) is consistent with its

399 origin from the phytyl side chain of chlorophyll *a* in phototrophic organisms, such as

400 phytoplankton and cyanobacteria (Rontani and Volkman, 2003). The highest concentration of

401 both phytol and phytane in layer B may be indicative for the impact of purple sulfur bacteria,

402 containing the phytyl moiety in the bacteriochlorophyll *a* and *b* (Brooks *et al.*, 1969; Powell

403 and McKirdy, 1973), which presence can caused the reddish color of this layer.

404 Concerning the distribution of FFAs difference is observed in content of long-chain

405 homologues which is much higher in lower layers C and D. The CPI, calculated based on the

406 FFAs distribution revealed markedly higher contribution of even than odd FFAs homologues

407 and increased with depth, however much slightly than CPI calculated from *n*-alkanes,

408 displaying values from 0.17 (layer A) to 0.26 (layer D). The notable prevalence of C_{16} and C_{18}

409 saturated FFAs, associated with their monounsaturated counterparts 16:1 and 18:1 confirmed

410 the dominance of cyanobacterial taxa (Abed *et al.*, 2015). Predominance of C_{16}, C_{18} and C_{19}

411 compounds among short-chain FFAs (C_{12}-C_{20}) was also reported in microalgae, zooplankton

412 and other bacteria (Gutiérrez *et al.*, 2012), which presence is expected in studied area.

413 The prevalence of C_{29} sterols in the C_{27}-C_{29} sterol distribution observed in all layers

414 (Table 2), is usually attributed to impact of higher plants or brown and green algae. However

415 since the contribution of higher plants to studied math is negligible, the domination of C_{29}

416 sterols can be related to the impact of brown and green algae. C_{27}-C_{29} sterol distribution

417 showed decreasing trend in order C_{29}>C_{27}>C_{28} in the upper layers A and B and C_{29}>C_{28}>C_{27}

418 in the lower layers C and D (Table 2). The higher content of C_{27} homologue in layers A and B

419 can be attributed to higher contribution of photosynthetic red algae to the upper layers.

420   The layers also distinguish according to abundance of unsaturated stenols, and

421   saturated stanols. The higher proportion of stanols in layers B and C compared to layers A

422   and D (layer D contains very low concentration of steroids due to the low impact of

423   photosynthetic eukaryotic algae) can be evidence of preferential degradation of stenols which

424   are less resistant to degradation than stanols and/or microbially-mediated stenol to stanol

425   conversion (Boudou *et al.*, 1987). The latter assumption is consistent with higher abundance

426   of 5α(H)-cholestan-3-one in the layers B and C than in layer A (Table 2), which is known

427   intermediary in the stenol → stanol conversion in algal mats. More intense microbial activity

428   in layers B and C is consistent with considerably higher amount of hopanols (Table 1) in these

429   two layers.

430   The highest content of bishomohopanol in layer B is consistent with higher impact of

431   sulfate reducing bacteria, presumed also based on the hop-17(21)-ene/hop-22(29)-ene ratio

432   and proportion of HMW *n*-alkanes. Moreover, some works have been showed that

433   *Planctomycetes, Geobacter spp*. and *Desulfovibrio spp*. are capable for hopanoid production

434   (Sinninghe Damsté *et al.*, 2004; Fischer *et al.*, 2005; Härtner *et al.*, 2005; Blumenberg *et al.*,

435   2006, 2012). Therefore, the contribution from anaerobic bacteria in layer B and particularly

436   layer C can also not be excluded. The highest content of tetrahymanol in layers B and C can

437   be attributed to marine ciliate species, most of which are scuticociliates, a widespread group

438   of protozoa that feed mainly on bacteria (Harvey and McManus, 1991), and usually occur at

439   the interface between oxic and anoxic zones in stratified water columns (Sinninghe Damsté *et*

440   *al*., 1995).

441

Glycolipids and Phospholipids

443   Hexadecanoic acid ME was the most prominent compound in GLs fractions of all

444   samples, followed by *n*-18:0 ME in deeper layers B-D, whereas in layer A higher

445   concentration of *n*-15:0 and *n*-14:0 ME than *n*-18:0 ME is observed (Table 3). This result is

446   consistent with prevalence of *n*-16:0 free FA in all layers and the lowest abundance of *n*-18:0

447   free FA in neutral lipids fraction of layer A.

448   Branched (*anteiso-* and *iso-*) and monounsaturated FAMEs were detected in GLs

449   fractions of all layers with predominance of branched FAMEs in the layers B-D and

450   monounsaturated FAMEs in the layer A (Fig. 5; Table 3). Branched FAs are commonly

451   considered to be of bacterial origin, e.g. from sulfate-reducing bacteria (some of them could

452   also be abundant in the oxic zones of mats; Baumgartner *et al.*, 2006) or sulfur-reducing

453   bacteria (Kaneda, 1991; Rütters *et al.*, 2002). In contrast, purple sulfur bacteria

454   (*Chromatiaceae*) only biosynthesize straight-chain even-carbon-numbered FAs such as *n*-

455   16:1, *n*-16:0, *n*-18:1 and *n*-18:0 (Imhoff and Bias-lmhoff, 1995). Abundant *iso*-15:0 FA also

456   can be as an indication of a gram-positive community (Lechevalier, 1988; Navarrete *et al.*,

457   2000; Romano *et al.*, 2008; Bühring *et al.*, 2009), which are abundant in hypersaline

458   environments (Caton *et al.*, 2004; Ghozlan *et al.*, 2006). Therefore, the obtained results

459   suggest higher contribution of sulfate-reducing and purple sulfur bacteria to layer B, which

460   has also been supposed based on the highest content of HMW *n*-alkanes, hopanol and phytol

461   (Table 2), as well as the highest hop-17(21)-ene/hop-22(29)-ene ratio in this layer.

462   The greatest concentrations of monounsaturated FAMEs, *n*-16:1 and *n*-18:1 in layers

463   A and B are in agreement with contribution of *Microcoleus sp*. (Rütters *et al.*, 2002; Bühring

464   *et al.*, 2009), which was the dominant cyanobacterium in studied mat. The presence of w9

465   monoenoic FAME could be related to aerobic desaturase pathway common to all cells,

466   whereas the w7 FAMEs (Table 3) could be indicative for anaerobic desaturase pathway,

467   which is often a prokaryotic biochemical pathway (Edlund *et al.*, 1985). Higher w9/w7 ratio

468   in layers B and C than in layer A (Table 3) is consistent with higher concentration of

469   eukaryotic sterols in these two layers (Table 2).

470   The distribution of FAMEs in PLs fractions of all samples is very scarce (Fig. 6). This

471   could be explained by the fact that phospholipids are quickly degraded, ranging from minutes

472   to a few hours after cell death (Sato and Murata, 1988), which is also generally reflected

473   through the uniform low contribution of PLs fraction (c.a. 5 %; Fig. 3) to all layers.

474   According to (Bowman *et al.*, 1995; Hanson and Hanson, 1996; Boschker *et al.*, 1998)

475   the signature of phospholipid fatty acids can be used to distinguish type I mesophilic

476   methane-oxidizing bacteria, which predominantly contain a series of *n*-16:1 mono-unsaturated

477   PLFAs, from type II, which contain *n*-18:1 mono-unsaturated PLFAs. However, these

478   compounds were not detected. Therefore, the predominance of *n*-16:0 PLFA over *n*-18:0

479   PLFA (Fig. 6), except layer C, could be related to contribution of the sulfate-reducing bacteria

480   such as *Desulfomicrobium sp.* strain.

481

482   ***The Relation of Precursor Lipids from Microbial Mat to Geologic Biosignatures***

483   **n-Alkanes and Isoprenoid Aliphatic Alkanes**

484   The prevalence of short-chain *n*-alkanes over long once in source rock extracts and

485   petroleums, usually expressed via TAR ratio, TAR = (n-C_{27} + n-C_{29} + n-C_{31})/(n-C_{15} + n-C_{17} +

486   n-C_{19}) (Bourbonniere and Meyers, 1996) is related to predominant aquatic origin of precursor

487   OM and/or high maturity, whereas elevated content of long-chain homologues (C_{25}-C_{33}),

488   particularly the odd once, signifies the contribution of epicuticular waxes from land plants. As

489   shown here, cyanobacteria synthesizes a large amount of C_{17} *n*-alkane and C_{17} 1-*n*-alkene

490   which hydrogenation during burial would result in formation of C_{17} *n*-alkane. Furthermore,

491   distributions of free- and fatty acids bounded in glyco- and phospholipids of microbial mat are

492   characterized by sharp prevalence of C_{16} and C_{18} homologues (Figs. 5, 6; Table 3), whereas

493   C_{16} and C_{18} are the most abundant *n*-alkanols in all layers with exception of layer B (Table 2).

494   Mentioned lipids with normal hydrocarbon skeleton produce *n*-alkanes during burial via

495   defunctionalization. Fatty acids undergo decarboxylation which results in formation of n-

496   alkanes having one C-atom less; in such case C_{16} and C_{18} fatty acids will produce C_{15} and C_{17}

497   n-alkanes. Other mechanism, favored in reducing environment involves reduction of FA to n-

498   alcohol, dehydration to n-alkene and further hydrogenation to n-alkane, having the same

499   number of carbon atoms as initial fatty acid. In such case C_{16} and C_{18} fatty acids will form C_{16}

500   and C_{18} n-alkanes. The fate of n-alkanols in sedimentary records depends on redox settings. In

501   oxygenated environment they undergo oxidation to fatty acids which further decarboxylation

502   results in formation of n-alkane with one C-atom less, whereas in reducing environment n-

503   alkanols dehydrated to n-alkene and further hydrogenated into n-alkane, without change in

504   carbon atom number. Independently, of redox settings, the results obtained in this study reveal

505   that source rocks extracts and petroleums derived from microbial mat should dominate by

506   short-chain n-alkanes, with notable prevalence of C_{15}-C_{18} homologues. Furthermore,

507   distribution of C_{15}-C_{18} homologues along with some other biomarker parameters (e.g.

508   pristane/phytane ratio, distribution of C_{31}-C_{35} homohopanes, and abundance of gammacerane

509   and β-carotane, see later) can be indicative for redox settings. Namely, prevalence of C_{15} and

510   C_{17} over C_{16} and C_{18} n-alkanes can be indicative for rather oxidizing environment, whereas

511   prevalence of C_{16} and C_{18} may imply reducing settings. Additionally, distribution of mid- and

512   long-chain n-alkanes (C_{22}-C_{30}) in ancient samples can contribute to determination of redox

513   depositional settings. Namely, since C_{22}-C_{30} n-alkanols are also present in studied mat, the

514   prevalence of even n-alkane homologues in the range C_{22}-C_{30} in sedimentary OM would

515   signify reducing environment, whereas the prevalence of odd n-alkanes would typify

516   oxidizing settings. The result is concordance with literature data that petroleum derived from

517   carbonate source rocks in reducing environment are characterized by prevalence of even n-

518   alkane homologues in range C_{22}-C_{32}, resulting in CPI<1 (Peters *et al*., 2005 and references

519   therein).

520   As it has been already mentioned, the elevated content of long-chain, particularly odd

521   *n*-alkane homologues is usually related to impact of higher plants or certain non-marine algae

522   (e.g. *Botryococcus braunii rice A*) which may contribute to the C_{27}-C_{31} *n*-alkanes (Moldowan

523   *et al*., 1985; Derenne *et al*., 1988). However, since the highest content of HMW *n*-alkanes

524   (C_{22}–C_{31}) was observed in layer B, which is associated with greater contribution of *Spirulina*

525   (Franco *et al.,* 2016), and sulfate-reducing- and heterotrophic bacteria, the elevated content of

526   mid- and long-chain *n*-alkanes in source rocks extracts and petroleums derived from

527   carbonate sources may be indicative to mentioned bacterial sources. Furthermore, the increase

528   in content of HMW *n*-alkanes in the deepest layer D may be indicative for anoxygenic

529   phototrophic and heterotrophic bacteria.

530   Regular isoprenoids pristane (Pr) and phytane (Ph) are abundant components of source

531   rock extracts and petroleums. The main precursor of both components is the phytyl side chain

532   of chlorophyll *a* in phototrophic organisms and bacteriochlorophyll *a* and *b* in purple sulfur

533   bacteria (e.g. Brooks *et al*., 1969; Powell and McKirdy, 1973). The formation of phytane is

534   favored in reducing conditions, whereas formation of pristane is related to oxic environment.

535   Although phytol was present in all layers of mat, only phytane was detected in studied

536   samples, and no pristane was observed. The obtained result is consistent with data from

537   geological records, that high Pr/Ph (>3.0) indicates terrigenous organic matter input under

538   oxic conditions, while low values (<0.8) typify anoxic, commonly hypersaline or carbonate

539   environments (Peters *et al*., 2005).

540   The presence of β-carotane in source rocks extracts and crude oils was well

541   documented (Philp *et al*., 1992; Koopmans *et al*., 1997; Chen *et al*., 2003; Hopmans *et al*.,

542   2005). However, high concentrations of this biomarker are typical for anoxic lacustrine, or

543   highly restricted marine environments (Jiang and Fowler, 1986; Fu *et al*., 1990). The

544   identification of β-carotane in layers A and B is consistent with production of its precursors

545   by cyanobacteria in arid and hypersaline environments (Jiang and Fowler, 1986; Koopmans *et*

546   *al.*, 1997), whereas absence of β-carotane in layers C and D unambiguously confirmed fast

547   degradation of the carotenoid skeleton by heterotrophic bacteria, and its synthesis by aerobic

548   organisms.

549

550   **Pentacyclic Triterpenoids (Hopanes and Gammacerane)**

551   22,29,30-Trisnorhop-17(21)-ene, 17β(H)-22,29,30-trisnorhopane, hop-17(21)-ene,

552   hop-22(29)-ene (diploptene) and bishomohopanol, detected in studied samples, are precursors

553   of C_{27}, C_{30} and C_{32} hopanes, widespread in source rock extracts and petroleums. Hopanes

554   with 30 carbon atoms generally dominated in ancient samples, and such pattern is also evident

555   in math' precursor OM (Fig. 4). The scarce distribution of hopanoids in microbial mat in

556   comparison with ancient sedimentary OM, where they are usually present in the C_{27}-C_{35} range

557   is related to the fact that hopanoids are generally bounded into macromolecules via a larger

558   number of binding sites (particularly numerous hydroxyl groups) than other biomarkers

559   (Hofmann *et al.*, 1991; Richnow *et al.*, 1991; Rohmer, 1993). This may lead to their

560   preferential incorporation into macromolecules, during very early diagenesis, and their

561   retention in bound fractions up to cracking in the oil window stage (Hofmann *et al.*, 1991;

562   Bowden *et al.*, 2006). On the other hand, C_{30} hop-17(21)-ene, C_{30} hop-22(29)-ene, C_{27}

563   22,29,30-trisnorhop-17(21)-ene and C_{27} 17β(H)-22,29,30-trisnorhopane do not possess

564   hydroxyl groups and consequently remained free or have been weakly adsorbed on the OM

565   and therefore has been easily detected in microbial mat. The conformation of our assumption

566   is the presence of full series of hopanoids typical for geological records observed in liquid

567   products obtained by hydropyrolysis of studied microbial mat (Franco *et al.*, 2016).

568   Tetrahymanol, detected in all layers (Table 2) is the main precursor of gammacerane

569   in source rocks and petroleums. Although present at least in trace amounts in most source

570 rock extracts and petroleums, large amount of gammacerane is generally related to highly

571 reducing, hypersaline conditions during deposition of the OM (Moldowan *et al*., 1985; Fu *et*

572 *al*., 1986), which coincides with our results, particularly from layers B and C. Moreover, high

573 content of gammacerane in carbonate derived source rocks and petroleums is usually

574 associated with elevated content of phytane (e.g. low pristane/phytane ratio), and precursors

575 of both compounds (tetrahymanol and phytol; Table 2), as well as phytane were identified in

576 all layers, whereas pristane was absent.

577

578 **Steroids**

579   The distribution of $5\alpha(H)14\alpha(H)17\alpha(H)20(R)$ C_{27}-C_{29} regular steranes is routine

580 parameter used in the evaluation of the sedimentary OM type. It is based on the observation

581 that C_{27} steranes originate dominantly from marine plankton and red algae (Huang and

582 Meinschein, 1979; Schwark and Empt, 2006), C_{28} steranes from yeast, fungi, plankton and

583 algae (Volkman, 2003), and C_{29} homologues from higher plants (Volkman, 1986), and brown

584 and green algae (Volkman, 2003). Marine environments are generally characterized by

585 prevalence of C_{27} or C_{29} sterane homologues, which is in agreement with distribution of

586 precursor C_{27}-C_{29} sterols observed in studied mat, since conversion of sterols into steranes

587 during geothermal maturation does not change a total number of carbon atoms in the

588 molecule.

589

590   **CONCLUSIONS**

591   The studied hypersaline mat has a flat dark pigmented green surface and internally

592 was subdivided into 4 different colors layers (A-D). The top of mat showed a green layer A

593 (0.5 cm), followed by a reddish brown layer B (0.5-1.5 cm), a dark brown greenish (1.5-3.0

594 cm) layer C, and a thicker bottom brown layer D (3.0-6.0 cm). Cyanobacterial taxa dominate

595 the biomass with a diversity of the 16 morphospecies in which *Microcoleus chthonoplastes*

596   prevailed. Based on the studied lipid classes contribution of sulfate-reducing bacteria such as

597   *Desulfomicrobium sp.* strain, purple sulfur bacteria, as well as possible input of *Geobacter*

598   *spp.* and *Desulfovibrio spp.*, particularly in deeper layers, is also established.

599   Notable decrease in total extractable lipids yield from A to D layer indicates that lipid

600   synthesis is much more intense by photosynthesizing cyanobacteria than by anaerobic

601   microorganisms. The content of PLs was uniform and very low (<5%) in all layers confirming

602   extremely quick degradation (from minutes to a few hours) after cell death. Therefore, layers

603   can be more effectively distinguishing based on composition of NLs and GLs than

604   composition of PLs. GLs that are accumulated as energy source, following by NLs were most

605   abundant in all layers indicating the medium which is characterized by excess of the carbon

606   source and limitation of microorganisms' growth by the nitrogen source.

607   The lipids composition showed adequate capability for distinguishing individual layers

608   within microbial mat. The NLs/GLs ratio decreases from layer A to D. Among the studied

609   lipid classes, the observed layers mostly differ according to amount of high molecular weight

610   *n*-alkanes and long-chain (C_{21}-C_{30}) *n*-alkanols, content of phytol, hopanol and sterols, the

611   stanol/stenol ratio, content of branched FAs in the GLs fraction, as well as w9/w7 FA ratio of

612   the GLs fraction. All mentioned parameters generally increase with depth, being commonly

613   the highest in layer B and implying a greater contribution of sulfate reducing- and purple

614   sulfur bacteria to this layer. Furthermore, based on the distribution of C_{27}-C_{29} sterols higher

615   impact of photosynthetic red algae is suggested in upper layers A and B, whereas the highest

616   content of tetrahymanol in layers B and C indicates elevated contribution of marine ciliate

617   species, feeding on bacteria, to these two layers. The greatest capability for hydrocarbons

618   synthesis is observed in layer B. Our results also imply microbially-mediated lipid diagenetic

619   alteration, particularly in layers B and C.

620   Comparison the composition of lipid classes in microbial mat and distributions of

621   biomarkers in ancient source rocks extracts and petroleums implies that precursor lipids

622   provide an essential data for the understanding of the transformation microbial OM during

623   sedimentation processes and its contribution to fossil records. This is particularly related to

624   distribution of *n*-alkanes, high abundance of phytane and gammacerane, as well as

625   distribution of C_{27}-C_{29} regular steranes in source rocks and petroleums derived from carbonate

626   hypersaline environments. The solely limitation in the direct connection of lipid composition

627   of microbial mats and fossil biomarkers concerns distribution of hopanes due to the fact that

628   hopanoids are preferentially bounded into macromolecules, during very early diagenesis, and

629   their more intense releasing occurs by cracking yet in the oil window stage.

630

633

634   **References**

635   Abed, R.M.M. and Garcia-Pichel, F., 2001, Long-term compositional changes after transplant

636   in a microbial mat cyanobacterial community revealed using a polyphasic approach:

637   Environmental Microbiology, v. 3, p. 53-62.

638   Abed, R.M.M., Klempová, T., Gajdoš, P. and Čertík, M., 2015, Bacterial diversity and fatty

639   acid composition of hypersaline cyanobacterial mats from an inland desert wadi: Journal of

640   Arid Environments, v. 115, p. 81-89.

641   Abed, R.M.M., Kohls, K., Schoon, R., Scherf, A.-K., Schacht, M., Palinska, K.A., Al-

642   Hassani, H., Hamza, W., Rullkötter, J. and Golubic, S., 2008, Lipid biomarkers, pigments

643   and cyanobacterial diversity of microbial mats across intertidal flats of the arid coast of the

644   Arabian Gulf (Abu Dhabi, UAE): FEMS Microbiology Ecology, v. 65, p. 449-462.

645 Allen, M.A., Neilan, B.A., Burns, B.P., Jahnke, L.L. and Summons, R.E., 2010, Lipid

646 biomarkers in Hamelin Pool microbial mats and stromatolites: Organic Geochemistry, v.

647 41, p. 1207-1218.

648 Alvarez, H.M., 2003, Relationship between β-oxidation pathway and the hydrocarbon-

649 degrading profile in actinomycetes bacteria: International Biodeterioration &

650 Biodegradation, v 52, p. 35-42.

651 Alvarez, H. and Steinbüchel, A., 2002, Triacylglycerols in prokaryotic microorganisms.

652 Applied Microbiology and Biotechnology, v. 60, p. 367-376.

653 Banerjee, A., Sharma, R., Chisti, Y and Banerjee, U.C., 2002, Botryococcus braunii: A

654 Renewable Source of Hydrocarbons and Other Chemicals: Critical Reviews in

655 Biotechnology, v. 22, p. 245-279.

656 Baumgartner, L.K., Reid, R.P., Dupraz, C., Decho, A.W., Buckley, D.H., Spear, J.R.,

657 Przekop, K.M. and Visscher, P.T., 2006, Sulfate reducing bacteria in microbial mats:

658 Changing paradigms, new discoveries: Sedimentary Geology, v. 185, p. 131-145.

659 Blumenberg, M., Krüger, M., Nauhaus, K., Talbot, H.M., Oppermann, B.I., Seifert, R., Pape,

660 T. and Michaelis, W., 2006, Biosynthesis of hopanoids by sulfate-reducing bacteria (genus

661 Desulfovibrio): Environmental Microbiology, v. 8, p. 1220-1227.

662 Blumenberg, M., Thiel, V., Riegel, W., Kah, L.C. and Reitner, J., 2012, Biomarkers of black

663 shales formed by microbial mats, Late Mesoproterozoic (1.1Ga) Taoudeni Basin,

664 Mauritania: Precambrian Research, v. 196-197, p. 113-127.

665 Boschker, H.T.S., Nold, S.C., Wellsbury, P., Bos, D., de Graaf, W., Pel, R., Parkes, R.J. and

666 Cappenberg, T.E., 1998, Direct linking of microbial populations to specific

667 biogeochemical processes by 13C-labelling of biomarkers: Nature, v. 392, p. 801-805.

668   Boudou, J.P., Boulègue, J., Maléchaux, L., Nip, M., de Leeuw, J.W. and Boon, J.J., 1987,

669   Identification of some sulphur species in a high organic sulphur coal: Fuel, v. 66, p. 1558-

670   1569.

671   Boudou, J.P., Trichet, J., Robinson, N. and Brassell, S.C., 1986, Lipid composition of a

672   Recent Polynesian microbial mat sequence: Organic Geochemistry, v. 10, p. 705-709.

673   Bourbonniere, R.A. and Meyers, P.A., 1996, Sedimentary geolipid records of historical

674   changes in the watersheds and productivities of Lakes Ontario and Erie: Limnology and

675   Oceanography, v. 41, p. 352-359.

676   Bowden, S.A., Farrimond, P., Snape, C.E. and Love, G.D., 2006, Compositional differences

677   in biomarker constituents of the hydrocarbon, resin, asphaltene and kerogen fractions: An

678   example from the Jet Rock (Yorkshire, UK): Organic Geochemistry, v. 37, p. 369-383.

679   Bowman, J.P., Sly, L.I. and Stackebrandt, E., 1995, The Phylogenetic Position of the Family

680   Methylococcaceae: International Journal of Systematic and Evolutionary Microbiology, v.

681   45, p. 182-185.

682   Brooks, J.D., Gould, K. and Smith, J.W., 1969, Isoprenoid hydrocarbons in coal and

683   petroleum: Nature, v. 222, p. 257-259.

684   Bühring, S.I., Smittenberg, R.H., Sachse, D., Lipp, J.S., Golubic, S., Sachs, J.P., Hinrichs, K.-

685   U. and Summons, R.E., 2009, A hypersaline microbial mat from the Pacific Atoll

686   Kiritimati: insights into composition and carbon fixation using biomarker analyses and a

687   13C-labeling approach: Geobiology, v. 7, p. 308-323.

688   Caton, T.M., Witte, L.R., Ngyuen, H.D., Buchheim, J.A., Buchheim, M.A. and Schneegurt,

689   M.A., 2004, Halotolerant aerobic heterotrophic bacteria from the Great Salt Plains of

690   Oklahoma: Microbial Ecology, v. 48, p. 449-462.

691 Chen, J., Liang, D., Wang, X., Zhong, N., Song, F., Deng, C., Shi, X., Jin, T. and Xiang, S.,

692   2003, Mixed oils derived from multiple source rocks in the Cainan oilfield, Junggar Basin,

693   Northwest China. Part I: genetic potential of source rocks, features of biomarkers and oil

694   sources of typical crude oils: Organic Geochemistry, v. 34, p. 889-909.

695 Damazio, C.M. and Silva E Silva, L.H., 2006, Cianobactérias em esteiras microbianas

696   coloformes da lagoa pitanguinha, Rio de Janeiro, Brasil: Revista Brasileira de

697   Paleontologia, v. 9, p. 165-170.

698 Derenne, S., Largeau, C., Casadevall, E. and Connan, J., 1988, Comparison of torbanites of

699   various origins and evolutionary stages. Bacterial contribution to their formation. Cause of

700   lack of botryococcane in bitumens: Organic Geochemistry, v. 12, p. 43-59.

701 Dijkman, N.A., Boschker, H.T.S., Stal, L.J. and Kromkamp, J.C., 2010, Composition and

702   heterogeneity of the microbial community in a coastal microbial mat as revealed by the

703   analysis of pigments and phospholipid-derived fatty acids: Journal of Sea Research, v. 63,

704   p. 62-70.

705 Dobson, G., Ward, D.M., Robinson, N. and Eglinton, G., 1988, Biogeochemistry of hot spring

706   environments: Extractable lipids of a cyanobacterial mat: Chemical Geology, v. 68, p. 155-

707   179.

708 Edlund, A., Nichols, P.D., Roffey, R. and White, D.C., 1985, Extractable and

709   lipopolysaccharide fatty acid and hydroxy acid profiles from Desulfovibrio species:

710   Journal of Lipid Research, v. 26, p. 982-988.

711 Fischer, W.W., Summons, R.E. and Pearson, A., 2005, Targeted genomic detection of

712   biosynthetic pathways: anaerobic production of hopanoid biomarkers by a common

713   sedimentary microbe: Geobiology, v. 3, p. 33-40.

714 Fourcans, A., de Oteyza, T.G., Wieland, A., Sole, A., Diestra, E., van Bleijswijk, J., Grimalt,

715   J.O., Kuhl, M., Esteve, I., Muyzer, G., Caumette, P. and Duran, R., 2004, Characterization

716 of functional bacterial groups in a hypersaline microbial mat community (Salins-de-
717 Giraud, Camargue, France): FEMS Microbiology Ecology, v. 51, p. 55-70.

718 Franco, N., Mendonça Filho, J.G., Silva, T.F., Stojanović, K., Fontana, L.F., Carvalhal-
719 Gomes, S.B.V., Silva, F.S. and Furukawa, G.G., 2016, Geochemical characterization of the
720 hydrous pyrolysis products from a recent cyanobacteria-dominated microbial mat:
721 Geologica Acta, v. 14, p. 385-401.

722 Fu, J., Sheng, G., Peng, P., Brassell, S., Eglinton, G. and Jigang, J., 1986, Peculiarities of salt
723 lake sediments as potential source rocks in China: Organic Geochemistry, v. 10, p. 119-
724 126.

725 Fu, J., Sheng, G., Xu, J., Eglinton, G., Gowar, A.P., Jia, R. and Fan, S., 1990, Application of
726 biological markers in assessment of paleoenvironments of Chinese non-marine sediments:
727 Organic Geochemistry, v. 16, p. 769-779.

728 Garcia-Pichel, F., Prufert-Bebout, L. and Muyzer, G., 1996, Phenotypic and phylogenetic
729 analyses show Microcoleus chthonoplastes to be a cosmopolitan cyanobacterium: Applied
730 and Environmental Microbiology, v. 62, p. 3284-3291.

731 Ghozlan, H., Deif, H., Kandil, R.A. and Sabry, S., 2006, Biodiversity of moderately
732 halophilic bacteria in hypersaline habitats in Egypt: The Journal of General and Applied
733 Microbiology, v. 52, p. 63-72.

734 Gillan, F.T. and Sandstrom, M.W., 1985. Microbial lipids from a nearshore sediment from
735 Bowling Green Bay, North Queensland: The fatty acid composition of intact lipid
736 fractions: Organic Geochemistry, v. 8, p. 321-328.

737 Grimalt, J.O., de Wit, R., Teixidor, P. and Albaigés, J., 1992, Lipid biogeochemistry of
738 Phormidium and Microcoleus mats: Organic Geochemistry, v. 19, p. 509-530.

739   Gutiérrez, M.H., Pantoja, S. and Lange, C.B., 2012, Biogeochemical significance of fatty acid

740   distribution in the coastal upwelling ecosystem off Concepción (36°S), Chile: Organic

741   Geochemistry, v. 49, p. 56-67.

742   Hanson, R.S. and Hanson, T.E., 1996, Methanotrophic bacteria: Microbiological Reviews, v.

743   60, p. 439-471.

744   Härtner, T., Straub, K.L. and Kannenberg, E., 2005, Occurrence of hopanoid lipids in

745   anaerobic Geobacter species: FEMS Microbiology Letters, v. 243, p. 59-64.

746   Harvey, H.R. and McManus, G.B., 1991, Marine ciliates as a widespread source of

747   tetrahymanol and hopan-3β-ol in sediments: Geochimica et Cosmochimica Acta, v. 55, p.

748   3387-3390.

749   Hofmann, I.C., Hutchinson, J., Robson, J.N., Chicarelli, M.I. and Maxwell, J.R., 1991,

750   Evidence for sulphide links in a crude oil asphaltene and kerogens from reductive cleavage

751   by lithium in ethylamine: Organic Geochemistry, v. 19, p. 371-387.

752   Hopmans, E.C., Schouten, S., Rijpstra, W.I.C. and Sinninghe Damsté, J.S., 2005,

753   Identification of carotenals in sediments: Organic Geochemistry, v. 36, p. 485-495.

754   Horodyski, R.J. and Bloeser, B., 1977, Laminated algal mats from a coastal lagoon, Laguna

755   Mormona, Baja California, Mexico: Journal of Sedimentary Research, v. 47, p. 680-696.

756   Huang, W-Y. and Meinschein, W.G., 1979, Sterols as ecological indicators: Geochimica et

757   Cosmochimica Acta, v. 43, p. 739-745.

758   Imhoff, J.F. and Bias-lmhoff, U. 1995, Lipids, Quinones and Fatty Acids of Anoxygenic

759   Phototrophic Bacteria, in Blankenship, R.E., Madigan, M.T. and Bauer, C.E., eds.,

760   Anoxygenic Photosynthetic Bacteria: Springer, Dordrecht, Netherlands, p. 179-205.

761   Jiang, Z.S. and Fowler, M.G., 1986, Carotenoid-derived alkanes in oils from northwestern

762   China: Organic Geochemistry, v. 10, p. 831-839.

763 Jonkers, H.M., Ludwig, R., De Wit, R., Pringault, O., Muyzer, G., Niemann, H., Finke, N.

764   and De Beer, D., 2003, Structural and functional analysis of a microbial mat ecosystem

765   from a unique permanent hypersaline inland lake: 'La Salada de Chiprana' (NE Spain):

766   FEMS Microbiology Ecology, v. 44, p. 175-189.

767 Kaneda, T., 1991, Iso- and anteiso-fatty acids in bacteria: biosynthesis, function, and

768   taxonomic significance: Microbiological Reviews, v. 55, p. 288-302.

769 Kates, M. 1972, Ether-linked lipids in extremely halophilic bacteria, in Snyder, F., ed., Ether

770   Lipids Chemistry and Biology: Academic Press, p. 351-398.

771 Kaur, G., Mountain, B.W., Hopmans, E.C. and Pancost, R.D., 2011, Relationship between

772   lipid distribution and geochemical environment within Champagne Pool, Waiotapu, New

773   Zealand: Organic Geochemistry, v. 42, p. 1203-1215.

774 Knoppers, B. and Kjerfve, B., 1999, Coastal Lagoons of Southeastern Brazil: Physical and

775   Biogeochemical Characteristics, in Perillo, G.M.E., Piccolo, M.C. and Pino-Quivira M.,

776   eds., Estuaries of South America: Their Geomorphology and Dynamics: Springer, Berlin,

777   Heidelberg, p. 35-66.

778 Koopmans, M.P., de Leeuw, J.W. and Sinninghe Damsté, J.S., 1997, Novel cyclised and

779   aromatised diagenetic products of β-carotene in the Green River Shale: Organic

780   Geochemistry, v. 26, p. 451-466.

781 Laut, L., Martins, M.V.A., Frontalini, F., Ballalai, J.M., Belart, P., Habib, R., Fontana, L.F.,

782   Clemente, I.M.M.M., Lorini, M.L., Mendonça Filho, J.G., Laut, V.M., and Figueiredo,

783   M.d.S.L., 2017, Assessment of the trophic state of a hypersaline-carbonatic environment:

784   Vermelha Lagoon (Brazil): PLOS ONE, v. 12, p. e0184819.

785 Lechevalier, H., 1988, Chemotaxonomic use of lipids - an overview: Microbial Lipids, v. 1, p.

786   869-902.

787   Lechevalier, M.P. and Moss, C.W., 1977, Lipids in Bacterial Taxonomy - A Taxonomist's

788   View: CRC Critical Reviews in Microbiology, v. 5, p. 109-210.

789   Lehtonen, K. and Ketola, M., 1993, Solvent-extractable lipids of Sphagnum, Carex, Bryales

790   and Carex-Bryales peats: content and compositional features vs. peat humification:

791   Organic Geochemistry, v. 20, p. 363-380.

792   Moldowan, J.M., Seifert, W.K. and Gallegos, E.J., 1985, Relationship between petroleum

793   composition and depositional environment of petroleum source rocks: American

794   Association of Petroleum Geologists Bulletin, v. 69, p. 1255-1268.

795   Moreira, N.F., Walter, L.M., Vasconcelos, C., McKenzie, J.A. and McCall, P.J., 2004, Role

796   of sulfide oxidation in dolomitization: Sediment and pore-water geochemistry of a modern

797   hypersaline lagoon system: Geology, v. 32, p. 701-704.

798   Navarrete, A., Peacock, A., Macnaughton, S.J., Urmeneta, J., Mas-Castellà, J., White, D.C.

799   and Guerrero, R., 2000, Physiological Status and Community Composition of Microbial

800   Mats of the Ebro Delta, Spain by Signature Lipid Biomarkers: Microbial Ecology, v. 39, p.

801   92-99.

802   Nytoft, H.P., 2011, Novel side chain methylated and hexacyclic hopanes: Identification by

803   synthesis, distribution in a worldwide set of coals and crude oils and use as markers for

804   oxic depositional environments: Organic Geochemistry, v. 42, p. 520-539.

805   Ourisson, G. and Rohmer, M., 1992, Hopanoids. 2. Biohopanoids: a novel class of bacterial

806   lipids: Accounts of Chemical Research, v. 25, p. 403-408.

807   Pagès, A., Grice, K., Ertefai, T., Skrzypek, G., Jahnert, R. and Greenwood, P., 2014, Organic

808   geochemical studies of modern microbial mats from Shark Bay: Part I: Influence of depth

809   and salinity on lipid biomarkers and their isotopic signatures: Geobiology v. 12, p. 469-

810   487.

811   Peters, K.E., Walters, C.C. and Moldowan, J.M., 2005, The Biomarker Guide, Volume 2:

812   Biomarkers and Isotopes in the Petroleum Exploration and Earth History: Cambridge

813   University Press, Cambridge, UK, 680 p.

814   Philp, R.P., Chen, J.H., Fu, J.M. and Sheng, G.Y., 1992, A geochemical investigation of crude

815   oils and source rocks from Biyang Basin, China: Organic Geochemistry, v. 18, p. 933-945.

816   Pierson, B.K., Valdez, D., Larsen, M., Morgan, E. and Mack, E.E., 1994, Chloroflexus-like

817   organisms from marine and hypersaline environments: Distribution and diversity:

818   Photosynthesis Research, p. 41, v. 35-52.

819   Piorreck, M. and Pohl, P., 1984, Formation of biomass, total protein, chlorophylls, lipids and

820   fatty acids in green and blue-green algae during one growth phase: Phytochemistry, v. 23,

821   p. 217-223.

822   Plet, C., Pagès, A., Holman, A.I., Madden, R.H.C. and Grice, K., 2018, From supratidal to

823   subtidal, an integrated characterisation of Carbla Beach shallow microbial mats (Hamelin

824   Pool, Shark Bay, WA): Lipid biomarkers, stable carbon isotopes and microfabrics:

825   Chemical Geology, v. 493, p. 338-352.

826   Powell, T.G. and McKirdy, D.M., 1973, Relationship between ratio of pristane to phytane,

827   crude oil composition and geological environment in Australia: Nature, v. 243, p. 37-39.

828   Ramos, V.M.C., Castelo-Branco, R., Leão, P.N., Martins, J., Carvalhal-Gomes, S., Sobrinho

829   da Silva, F., Mendonça Filho, J.G. and Vasconcelos, V.M., 2017, Cyanobacterial Diversity

830   in Microbial Mats from the Hypersaline Lagoon System of Araruama, Brazil: An In-depth

831   Polyphasic Study: Frontiers in Microbiology, v. 8, p. 1233.

832   Řezanka, T., Sokolov, M.Y. and Víden, I., 1990, Unusual and very-long-chain fatty acids in

833   Desulfotomaculum, a sulfate-reducing bacterium: FEMS Microbiology Ecology, v. 6, p.

834   231-237.

835   Řezanka, T., Zlatkin, I.V., Víden, I., Slabova, O.I. and Nikitin, D.I., 1991, Capillary gas

836   chromatography-mass spectrometry of unusual and very long-chain fatty acids from soil

837   oligotrophic bacteria: Journal of Chromatography A, v. 558, p. 215-221.

838   Richert, L., Golubic, S., Le guédès, R., Hervé, A. and Payri, C., 2006, Cyanobacterial

839   populations that build 'kopara' microbial mats in Rangiroa, Tuamotu Archipelago, French

840   Polynesia: European Journal of Phycology, v. 41, p. 259-279.

841   Richnow, H.H., Jenisch, A. and Michaelis, W., 1991, Structural investigations of sulphur-rich

842   macromolecular oil fractions and a kerogen by sequential chemical degradation: Organic

843   Geochemistry, v. 19, p. 351-370.

844   Riding, R., 2000, Microbial carbonates: the geological record of calcified bacterial–algal mats

845   and biofilms: Sedimentology, v. 47, p. 179-214.

846   Rocha, L. and Borgui, L., 2017, Análise de Microbiofácies das Esteiras Microbianas da Lagoa

847   Pitanguinha (Região dos Lagos, RJ, Brasil): Anuário do Instituto de Geociências – UFRJ,

848   v. 40, p. 191-205.

849   Rohmer, M., 1993, The biosynthesis of triterpenoids of the hopane series in the Eubacteria: A

850   mine of new enzyme reactions: Pure and Applied Chemistry, v. 65, p. 1293-1298.

851   Rohmer, M., Bouvier-Nave, P. and Ourisson, G., 1984, Distribution of Hopanoid Triterpenes

852   in Prokaryotes: Microbiology, v. 130, p. 1137-1150.

853   Romano, I., Finore, I., Nicolaus, G., Huertas, F.J., Lama, L., Nicolaus, B. and Poli, A., 2008,

854   Halobacillus alkaliphilus sp. nov., a halophilic bacterium isolated from a salt lake in Fuente

855   de Piedra, southern Spain: International Journal of Systematic and Evolutionary

856   Microbiology, v. 58, p. 886-890.

857   Rontani, J.-F. and Volkman, J.K., 2003, Phytol degradation products as biogeochemical

858   tracers in aquatic environments: Organic Geochemistry, v. 34, p. 1-35.

859 Rontani, J.-F. and Volkman, J.K., 2005, Lipid characterization of coastal hypersaline

860 cyanobacterial mats from the Camargue (France): Organic Geochemistry, v. 36, p. 251-

861 272.

862 Rütters, H., Sass, H., Cypionka, H. and Rullkötter, J., 2002, Phospholipid analysis as a tool to

863 study complex microbial communities in marine sediments: Journal of Microbiological

864 Methods, v. 48, p. 149-160.

865 Sánchez, O., Ferrera, I., Vigués, N., Oteyza, T.G.d., Grimalt, J. and Mas, J., 2006, Role of

866 cyanobacteria in oil biodegradation by microbial mats: International Biodeterioration &

867 Biodegradation, v. 58, p. 186-195.

868 Sato, N. and Murata, N., 1988, Membrane lipids: Methods in Enzymology, v. 167, p. 251-

869 259.

870 Scherf, A.-K. and Rullkötter, J., 2009, Biogeochemistry of high salinity microbial mats – Part

871 1: Lipid composition of microbial mats across intertidal flats of Abu Dhabi, United Arab

872 Emirates: Organic Geochemistry, v. 40, p. 1018-1028.

873 Schwark, L. and Empt, P., 2006, Sterane biomarkers as indicator of palaeozoic algal evolution

874 and extinction events: Palaeogeography, Palaeoclimatology, Palaeoecology, v. 240, p. 225-

875 236.

876 Silva E Silva, L.H. and Carvalhal, S.B.V., 2005, Biolaminóides Calcários Holocênicos da

877 Lagoa Vermelha, Brasil: Anuário do Instituto de Geociências UFRJ, v. 28, p. 59-70.

878 Silva E Silva, L.H., Damazio, C.M. and Iespa, A.A.C., 2005, Registro de biolaminóides

879 poligonais na lagoa de Araruama, Estado do Rio de Janeiro, Brasil: Revista de Geologia, v.

880 18, p. 153-158.

881 Silva E Silva, L.H., Senra, M.C.E., Faruolo, T.C.L.M., Carvalhal, S.B.V., Alves, S.A.P.M.N.,

882 Damazio, C.M., Shimizu, V.T.A., Santos, R.C. and Iespa, A.A.C., 2004, Composição

883   paleobiológica e tipos morfológicos das construções estromatolíticas da Lagoa Vermelha,

884   RJ, Brasil: Revista Brasileira de Paleontologia, v. 7, p. 193-198.

885 Silva, L.H.d.S.e. and Carvalhal, S.B.V., 2005, Biolaminóides Calcários Holocênicos: o Caso

886   da Lagoa Vermelha, Brasil: Anuário do Instituto de Geociências UFRJ, v. 28, p. 59-70.

887 Sinninghe Damsté, J.S., Kenig, F., Koopmans, M.P., Köster, J., Schouten, S., Hayes, J.M. and

888   de Leeuw, J.W., 1995, Evidence for gammacerane as an indicator of water column

889   stratification: Geochimica et Cosmochimica Acta, v. 59, p. 1895-1900.

890 Sinninghe Damsté, J.S., Rijpstra, W.I.C., Schouten, S., Fuerst, J.A., Jetten, M.S.M. and

891   Strous, M., 2004, The occurrence of hopanoids in planctomycetes: implications for the

892   sedimentary biomarker record: Organic Geochemistry, v. 35, p. 561-566.

893 Stolz, J.F. 2000, Structure of Microbial Mats and Biofilms, in Riding, R.E. and Awramik,

894   S.M. eds., Microbial Sediments: Springer-Verlag, Berlin, Heidelberg, p. 1-8.

895 Summons, R.E., Jahnke, L.L. and Roksandic, Z., 1994, Carbon isotopic fractionation in lipids

896   from methanotrophic bacteria: Relevance for interpretation of the geochemical record of

897   biomarkers: Geochimica et Cosmochimica Acta, v. 58, p. 2853-2863.

898 Thiel, V., Merz-Preiß, M., Reitner, J. and Michaelis, W., 1997, Biomarker studies on

899   microbial carbonates: Extractable lipids of a calcifying Cyanobacterial mat (Everglades,

900   USA): Facies, v. 36, p. 163-172.

901 Tissot, B.P. and Welte, D.H., 1984, Petroleum Formation and Occurrence, 2nd Edition:

902   Springer-Verlag, Heidelberg, Germany, 669 p.

903 van Gemerden, H., 1993, Microbial mats: A joint venture: Marine Geology, v. 113, p. 3-25.

904 van Lith, Y., Vasconcelos, C., Warthmann, R., Martins, J.C.F. and McKenzie, J.A., 2002,

905   Bacterial sulfate reduction and salinity: two controls on dolomite precipitation in Lagoa

906   Vermelha and Brejo do Espinho (Brazil): Hydrobiologia, v. 485, p. 35-49.

907 Vasconcelos, C., Warthmann, R., McKenzie, J.A., Visscher, P.T., Bittermann, A.G. and van

908   Lith, Y., 2006, Lithifying microbial mats in Lagoa Vermelha, Brazil: Modern Precambrian

909   relics?: Sedimentary Geology, v. 185, p. 175-183.

910 Venkatesan, M.I., 1988, Diploptene in Antarctic sediments: Geochimica et Cosmochimica

911   Acta, v. 52, p. 217-222.

912 Venkatesan, M.I., 1989, Tetrahymanol: Its widespread occurrence and geochemical

913   significance: Geochimica et Cosmochimica Acta, v. 53, p. 3095-3101.

914 Visscher, P.T., Prins, R.A. and van Gemerden, H., 1992, Rates of sulfate reduction and

915   thiosulfate consumption in a marine microbial mat: FEMS Microbiology Ecology, v. 9, p.

916   283-293.

917 Volkman, J.K., 1986, A review of sterol markers for marine and terrigenous organic matter:

918   Organic Geochemistry, v. 9, p. 83-99.

919 Volkman, J.K., 2003, Sterols in microorganisms: Applied Microbiology and Biotechnology,

920   v. 60, p. 496-506.

921 Volkman, J.K., Allen, D.I., Stevenson, P.L. and Burton, H.R., 1986, Bacterial and algal

922   hydrocarbons in sediments from a saline Antarctic lake, Ace Lake: Organic Geochemistry,

923   v. 10, p. 671-681.

924 Ward, D.M., Ferris, M.J., Nold, S.C. and Bateson, M.M., 1998, A Natural View of Microbial

925   Biodiversity within Hot Spring Cyanobacterial Mat Communities: Microbiology and

926   Molecular Biology Reviews, v. 62, p. 1353-1370.

927 Wolff, G.A., Ruskin, N. and Marshal, J.D., 1992, Biogeochemistry of an early diagenetic

928   concretion from the Birchi Bed (L. Lias, W. Dorset, UK): Organic Geochemistry, v. 19, p.

929   431-444.

930

931 **FIGURE CAPTIONS**

932

933 Figure 1. Map showing the location of Vermelha lagoon ("Lagoa Vermelha") on the

934 southeastern coast of the state of Rio de Janeiro, Brazil.

935

936 Figure 2. Polygonal mat from the Vermelha lagoon. (A) Detail map of the Vermelha lagoon

937 showing the E7 sampling site; (B) Microbial mats at the E7 site; (C-D) Transversal cut

938 showing inner laminations and color zonation.

939

940 Figure 3. Total extractable lipids (TELs) of microbial mat layers.

941 NLs – neutral lipids, GLs – glycolipids, PLs – phospholipids.

942

943 Figure 4. Partial mass chromatograms of m/z 191 showing hopanoids distribution.

944 1 – C_{27} 22,29,30-trisnorhop-17(21)-ene; 2 – C_{27} 17β(H)-22,29,30-trisnorhopane;

945 3 – C_{30} hop-17(21)-ene; 4 – C_{30} hop-22(29)-ene (diploptene).

946

947 Figure 5. Partial mass chromatograms of m/z 74 showing FAMEs profiles from GLs fractions.

948 Fatty acids are denoted as x:y, with x indicating number of carbon atoms and y giving the

949 number of double bonds; structural isomers are denoted by prefixes: n = normal, i = *iso*,

950 ai = *anteiso*, br = branched; additional methyl groups are noted with their position. A - D:

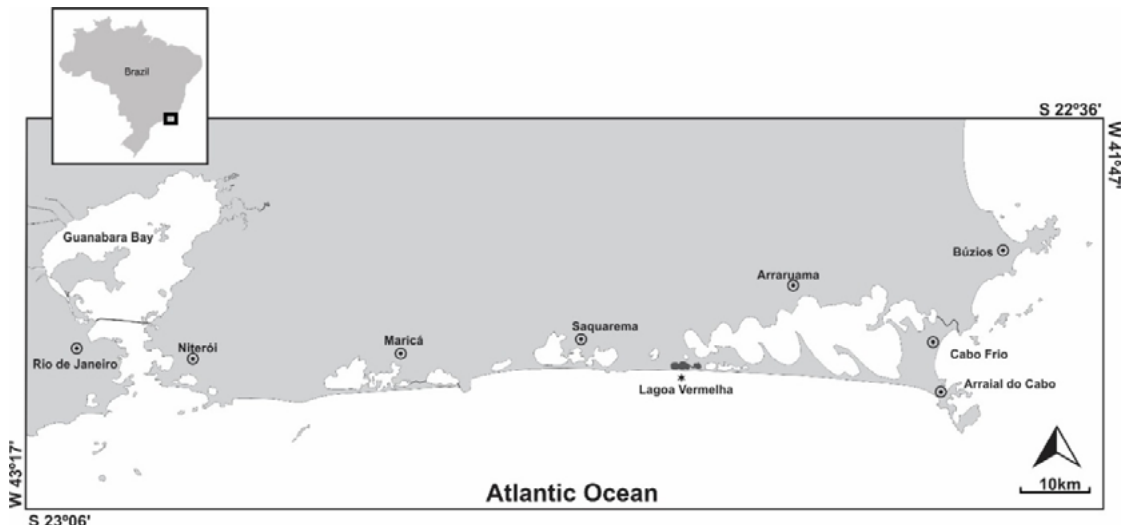951 layers from microbial mat sample.

952

953 Figure 6. Partial mass chromatograms of m/z 74 showing FAMEs profiles from PLs fractions.

954 Fatty acids are denoted as x:y, with x indicating number of carbon atoms and y giving the

955 number of double bonds. A - D: layers from microbial mat sample.
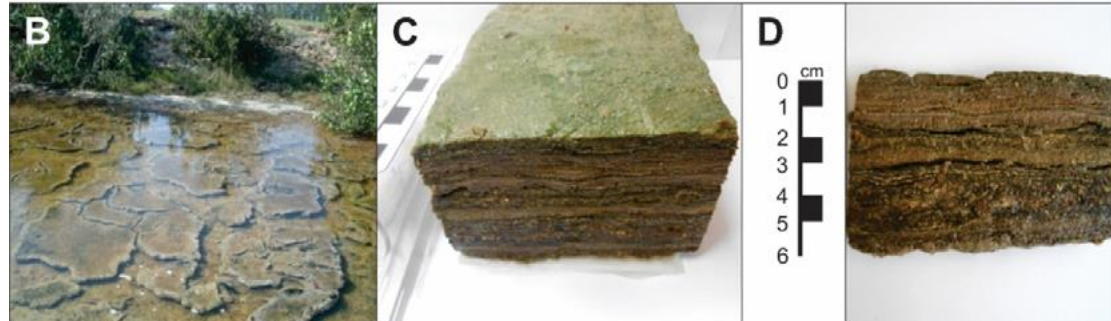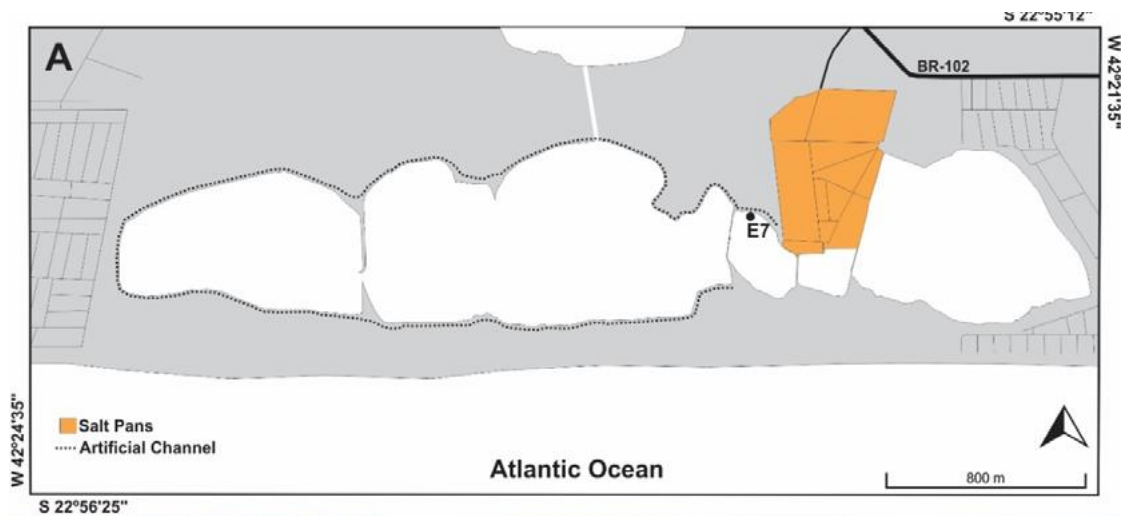
956

957

958
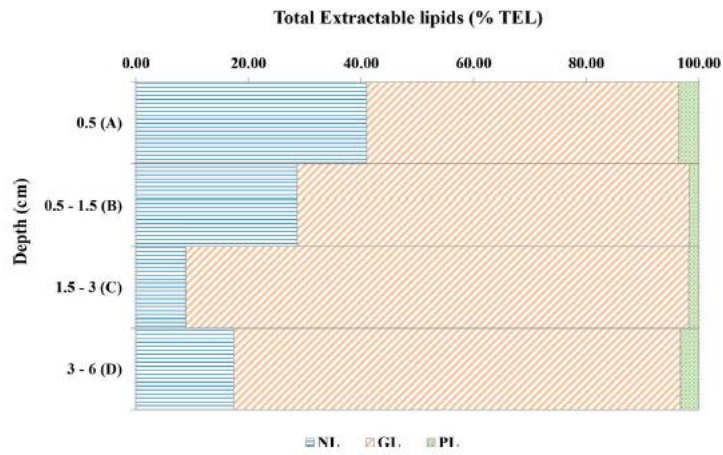959 Figure 1.
960
961
962
963

964
965 Figure 2.
966

967

968

Total Extractable lipids (% TEL)

969
970
971   Figure 3.

972
973
974
975

976
977
978   Figure 4.
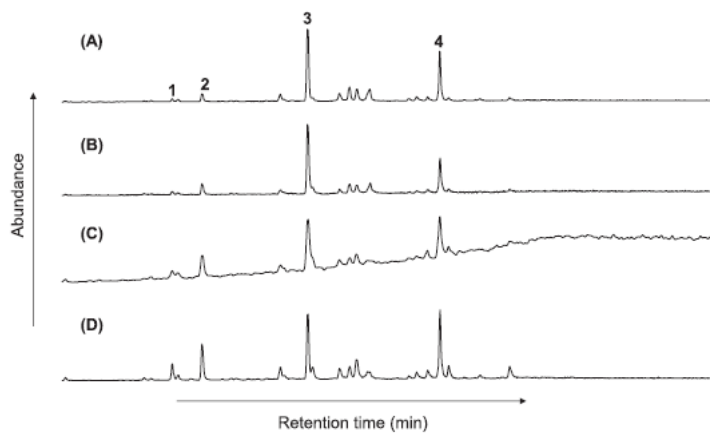
979
980
981
982
983
984
985
986
987
988
989
990
991
992
993
994
995

Figure 5.
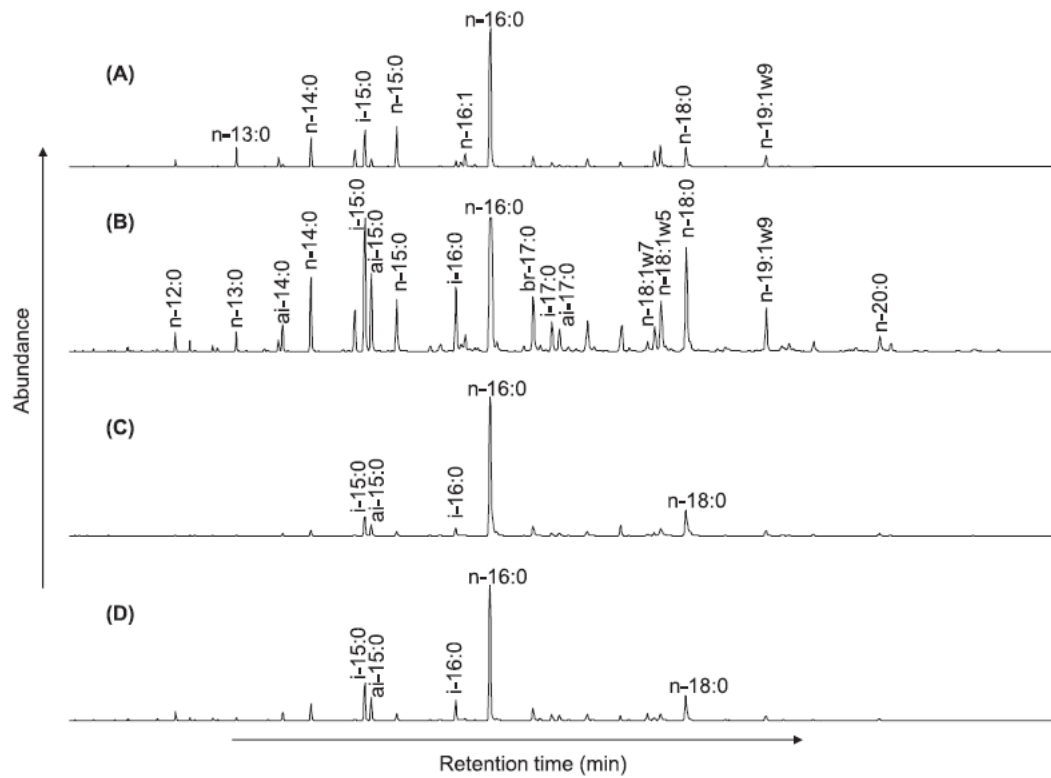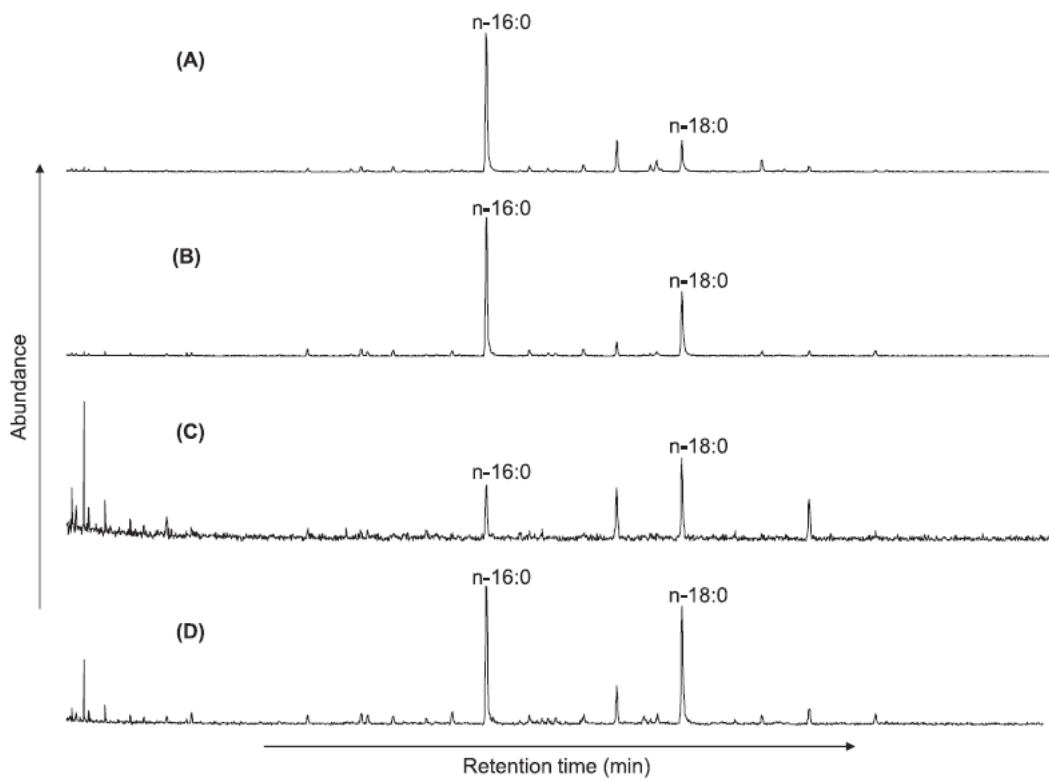
Figure 6.

1054
1055 Table 1. Concentrations (µg/g dry weight mat) of the isolated classes from neutral lipids

1056 fraction (quantification from GC-MS) in layers A-D

1057

Layer	Lipid component[*] (µg/g dry mat)					
(Depth, cm)	Hydrocarbons	FFAs	Alcohols	Sterols	Hopanols	Wax esters
A (0.5)	7.45	1234.73	22.08	11.18	1.75	1.30
B (0.5 - 1.5)	144.41	229.24	25.17	26.06	6.06	1.31
C (1.5 - 3)	2.72	32.24	15.06	21.26	3.66	0.41
D (3.0 - 6.0)	4.77	4.72	0.91	0.85	0.12	N.D.

1058 * – Obtained by summing concentrations of individual components; FFAs – Free fatty acids;

1059 N.D. – Not detected.

1060
1061
1062
1063
1064
1065
1066
1067
1068
1069
1070
1071
1072
1073
1074
1075
1076
1077
1078
1079
1080
1081
1082
1083
1084
1085
1086
1087
1088
1089

1090
1091 Table 2. Compositions of straight- and isoprenoid chain alcohols, steroids and triterpenoid

1092 alcohols of microbial mat

1093

Straight chain alcohols (µg/g dry mat)	A	B	C	D
n-14:0	0.55	0.47	0.19	0.01
n-15:0	1.58	0.70	0.24	0.01
n-16:0	2.39	1.75	0.83	0.06
n-17:0	1.00	0.70	0.41	0.01
n-18:1w9	0.61	0.28	0.38	0.02
n-18:0	2.86	2.21	1.68	0.15
n-20:0	2.40	2.30	1.40	0.14
n-21:0	0.13	N.D.	N.D.	N.D.
n-22:0	1.75	1.90	1.22	0.09
n-23:0	0.12	0.14	0.04	N.D.
n-24:0	0.93	2.29	2.70	0.12
n-26:0	0.80	2.17	1.15	0.06
n-28:0	1.68	2.51	0.79	0.11
n-30:0	1.20	1.61	0.90	0.07
Total straight chain alcohols (µg/g dry mat)	20.07	20.42	12.33	0.87
n-Alkanol maximum	*n*-18:0	*n*-28:0	*n*-24:0	*n*-18:0
Short-chain/long-chain *n*-alkanols	1.94	0.90	0.76	0.89
Branched chain (isoprenoid) alcohols (µg/g dry mat)	**A**	**B**	**C**	**D**
Isophytol	1.03	2.53	2.15	0.03
Phytol	0.98	2.22	0.58	0.01
Total branched chain alcohols (µg/g dry mat)	2.01	4.75	2.73	0.04
Steroids (µg/g dry mat)	**A**	**B**	**C**	**D**
5β(H)-Cholestan-3β-ol	0.13	0.61	0.16	N.D.
5β(H)-Cholestan-3α-ol	0.90	3.85	3.19	0.07
5α(H)-Cholestan-3-one	0.95	3.57	5.54	N.D.
Cholest-5-en-3β-ol	2.00	1.73	0.23	0.03
5α(H)-Cholestan-3β-ol	0.34	2.09	0.55	0.01
5β(H)-24-Methylcholestan-3α-ol	0.45	0.88	1.18	N.D.
24-Methylcholest-5-en-3β-ol	1.12	2.55	1.48	0.06
5α(H)-24-Methylcholestan-3β-ol	0.95	2.79	2.72	0.07
24-Ethylcholest-5,22(E)-dien-3β-ol	0.99	1.36	0.28	N.D.
Cycloartenol	0.55	1.98	0.13	N.D.
24-Ethylcholest-5-en-3β-ol	2.52	3.56	4.32	0.52
5α(H)-24-Ethylcholestan-3β-ol	1.22	4.67	7.03	0.09

	A	B	C	D
Total steroids (µg/g dry mat)	12.12	29.64	26.81	0.85
Total sterols (µg/g dry mat)	11.17	26.07	21.27	0.85
C_{27} Sterols (%)	31.73	34.37	19.54	12.94
C_{28} Sterols (%)	23.73	25.82	25.45	15.29
C_{29} Sterols (%)	44.54	39.81	55.01	71.76
ΣC_{27}-C_{29} unsaturated sterols (%)	6.63	9.20	6.31	0.61
ΣC_{27}-C_{29} saturated stanols (%)	3.99	14.89	14.83	0.24
Triterpenoid alcohols (µg/g dry mat)	**A**	**B**	**C**	**D**
Bishomohopanol	1.75	6.06	3.66	0.12
Tetrahymanol	0.91	2.06	2.72	0.02
Total triterpenoid alcohols (µg/g dry mat)	2.66	8.12	6.38	0.14

1094   N.D. – Not detected.
1095
1096
1097
1098
1099
1100
1101
1102
1103
1104
1105
1106
1107
1108
1109
1110
1111
1112
1113
1114
1115
1116
1117
1118
1119
1120
1121
1122
1123
1124
1125
1126
1127
1128

1129
1130 Table 3. FAMEs composition from glycoplipid fractions of microbial mat

1131

FAMEs from GLs (µg/g dry weight mat)			
Normal saturated	**A**	**B**	**C**	**D**
n-13:0	3.27	1.04	N.D.	0.54
n-14:0	5.66	6.00	1.69	4.66
n-15:0	8.76	4.6	1.59	2.20
n-16:0	43.17	24.73	54.90	44.16
n-18:0	5.30	10.82	14.12	9.68
Total	66.16	47.19	72.30	61.24
Branched	**A**	**B**	**C**	**D**
iso-14:0	1.68	0.77	N.D.	N.D.
anteiso-14:0	0.47	1.75	N.D.	1.99
iso-15:0	7.72	13.56	6.14	10.88
anteiso-15:0	1.62	6.69	3.28	6.29
iso-16:0	1.32	6.42	3.48	6.59
br-17:0	2.53	5.04	4.71	4.05
iso-17:0	1.03	2.58	1.42	2.13
anteiso-17:0	0.51	1.71	1.66	1.7
Total	16.88	38.52	20.69	33.63
Monounsaturated	**A**	**B**	**C**	**D**
16:1[*]	0.79	0.28	N.D.	N.D.
16:1w7	3.01	1.18	N.D.	N.D.
18:1w7	4.29	2.42	1.03	0.83
18:1w5	5.77	5.89	3.46	2.64
19:1w9	3.10	4.52	2.52	1.66
Total	16.96	14.29	7.01	5.13
19:1w9/(16:1w7+18:1w7)	0.42	1.26	2.45	2.00
19:1w9/18:1w7	0.72	1.87	2.45	2.00

1132 *n* – Normal saturated; *iso* – Iso branching; *anteiso* – Anteiso branching; br – Branched at unknown

1133 position; * – Unknown position of the double bond; N.D. – Not detected.

1134
1135

1136

1137

1138